IOSR Journal of Agriculture and Veterinary Science (IOSR-JAVS)
e-ISSN: 2319-2380, p-ISSN: 2319-2372. Volume 16, Issue 11 Ser. II (November. 2023), PP 01-09
www.iosrjournals.org

Establishment Of Micro-Discrete Element Model Of Corn Kernel Powdery Endosperm Based On SEM And PFC^{2D}

Mingjie Gao[1], Bolong Wang[1], Duanyang Geng[1], Guohai Zhang[1],Zhiyong Lin[1]
[1](*School of Agricultural Engineering and Food Science,Shandong University of Technology, Zibo ,China)*

Abstract:
The root cause of corn kernel crushing is due to microscopic mechanical damage within the corn kernel during harvest and subsequent processing, and macroscopic crushing occurs if the damaged corn is subjected to sustained force. In this study, the powdered endosperm of corn kernels is used as an example to establish its microscopic discrete element model to study the generation and evolution of microscopic cracks. By taking SEM images of the powdered endosperm of corn kernels, the microscopic morphology and particle gradation of the powdered endosperm fraction of corn kernels were obtained, and starch existed in the powdered endosperm in the form of particles, with diameters mainly in the range of 2~22 μm. The SEM image was used as a reference to establish a discrete element model of the powdery endosperm portion of the corn kernel using PFC^{2D}. The loading process of the model had four stages: initial, development, crack generation, and crack extension, and the peak stress on the loading plate was 28.5 MPa, which appeared in the crack generation stage, and the continued loading would lead to the rapid extension of the cracks. The stress-strain curves obtained in the loading process were basically consistent with those obtained in the powdered endosperm puncture experiments, which verified the validity of the modeling. This study provides a basic reference and solution for numerical modeling of microscopic discrete elements for biomaterials, and opens up a new approach to the study of micromechanical properties of biomaterials.

Keywords: *Corn powdery endosperm;discrete element model; PFC^{2D};starch granules; microstructure damage.*

Date of Submission: 18-11-2023 Date of Acceptance: 28-11-2023

I. Introduction

Corn is one of the three major food crops and today is widely grown in more than 160 countries, ranking first in global food crop production[1,2]. Corn is not only an important food crop in agriculture, but also an important raw material in industrial production, with a wide range of applications[3,4]. Changes in the quality of corn kernels will directly affect its storage time, damaged corn kernels are more prone to mold, and the moldy corn kernels will infect the surrounding kernels resulting in significant losses[5-8], therefore, exploring the mechanical properties of corn kernels to reduce the crushing rate of kernels in the harvesting and subsequent processing of maize has become a critically important issue. The root cause of corn kernel crushing is due to damage during harvesting or subsequent mechanical processing of corn kernels, which will produce microscopic cracks, and if the corn kernels are subjected to force again at this time, the original microscopic cracks will expand rapidly and gradually evolve into macroscopic cracks, leading to the eventual crushing of corn kernels [9,10].

According to the anatomical characteristics of the corn kernel, the corn kernel can be treated as a multibody system with three main components: horny endosperm, powdered endosperm, and germ, which have completely different mechanical properties due to the great differences in their composition and microstructure, and these three components account for about 94% of the overall composition of the corn kernel, which basically determines the mechanical properties of the corn kernel as a whole[11]. There are many methods for evaluating the mechanical properties of corn kernels, but according to the literature that has been published so far, there is no standard judging method that can be utilized, and at present, the most commonly used methods for testing the mechanical properties of corn kernels include biaxial compression experiments using a universal testing machine or a mass tester or combining with software such as Abaqus and Ansys to model the whole of the corn kernel and perform simulation analyses, in order to judge the overall modulus of elasticity of the corn kernel or the mechanical parameters such as the breaking force[12-15]. Such experiments were conducted on the whole corn kernel with uniform geometry, and the corn kernel was not divided into three parts: horny endosperm, powdered endosperm and germ for testing and analyzing, which resulted in the loss of its individual tissue properties. Currently, the stress-strain curves of different tissues of corn kernels are mainly obtained by puncture experiments to investigate the independent mechanical properties of each tissue[11].

In this paper, a new approach is taken to investigate the microscopic damage of corn kernels, taking the powdered endosperm of corn kernels as an example, taking SEM images of the powdered endosperm, observing its microscopic morphology, and using its actual morphology as a reference to build up its discrete elemental model by using PFC^{2D}, in order to investigate the generation and evolution of microscopic cracks in corn kernels. This study provides a basic reference and solution for the establishment of microscopic discrete elemental models for biomaterials, and also provides a new way to study the micromechanical properties of different tissues of maize kernels at a deeper level, which is of reference significance for the further study and reduction of mechanical damages to maize kernels caused by the application of external forces during and after harvesting.

II. Materials and methods

Corn kernel samples

The experiments were conducted with Zhengdan 958 corn variety, which is commonly grown in China, the kernels are yellow, half horsetooth type, with 20% moisture content, the average length of kernel is 13.65 mm, width is 8.23 mm, height is 4.16 mm, and the weight of 1,000 kernels is 300-350 g. Corn kernel samples were manually harvested and threshed in August 2022 from Jinan, Shandong province, and subsequently transported in self-sealing bags to the Laboratory. A simple test setup was built for simple screening of corn kernels due to macroscopic stress cracks that occur during natural drying. The test setup mainly consists of a metal box, a 60 watt light source, a mirror and a lens[15]. Corn kernels were placed at the focal point of the light source to observe the stress cracks, and the undamaged kernels were screened to take SEM images.

Sample preparation for SEM photography

Scanning electron microscope (SEM) is an electron beam-based microscopy technique used to observe and study the surface morphology and microstructure of samples, compared with traditional optical microscopes, SEM has higher resolution and magnification, and can provide more detailed image information, while the specimen preparation is easy, it is one of the most commonly used characterization and testing instruments in modern scientific research, and is widely used in the materials, chemistry, biology, and geology, etc.[16]. In order to utilize SEM to photograph the microstructure of the powdered endosperm of corn kernels, the samples used for SEM have to be produced, and the sample production is divided into two main parts: polishing and gold spraying treatment. First select the corn kernels screened in advance, truncate the corn kernels from the middle, exposing the powdery endosperm portion, due to the truncated fracture surface surface flatness is poor, it is necessary to polish the surface of the corn kernel fracture surface, respectively, select 100 to 2000 mesh sandpaper in turn on the fracture surface to polish the surface, in order to reduce the surface roughness of the fracture surface of the corn kernels. Then the corn kernel sample was sprayed with gold, in SEM, the electron beam needs to interact with the surface of the sample in order to produce an image, however, many samples, especially non-metallic samples, have low electrical conductivity, which can lead to the accumulation of charge on the surface of the sample due to the high energy of the electron beam, which can result in the problems such as drift of the electron beam, blurred image, or distortion, etc., in order to solve these problems, the gold spraying treatment can be used to increase the electrical conductivity of the surface of the corn kernel sample so that the preparation of the sample for the scanning electron microscope (SEM) shot is basically completed.

Microstructure morphology and particle size distribution of powdered endosperm

After completing the sample production, the sample was fixed on the base for photographing work. The scanning electron microscope (SEM) model Quanta 250 was used for the photographing, and the photographing voltage was 5kV, the working distance was 10.1786mm, the magnification was 2000, and the SEM image of the powdered endosperm of maize kernel was shown in Fig.1.

The main component of corn kernels is starch, followed by protein. Starch accounts for about 70% of the weight of mature corn kernels, and protein generally accounts for 10% to 14% of the mass of mature corn kernels. As can be seen in Fig.1, starch is present as granules in the powdered endosperm of the corn kernel, which is spherical in shape, with the granules arranged loosely and irregularly. Proteins are distributed in the spaces between the starch granules of corn kernels, which are irregular in shape and have a certain bonding effect on the starch granules. Although there are proteins between the starch granules, there are still some pores.

The granular gradation of starch granules can be obtained by observation of SEM images of powdered endosperm. Measurement of starch granule particle size in SEM images of powdered endosperm of corn kernels was carried out using ImageJ to calibrate the size of starch granules in the SEM images according to the given scale, the number of starch granule samples was 517, and the results of the measurements are shown in Fig.2. The diameters of starch granules ranged from 2 to 22 μm, but the majority of starch granules were concentrated in the size range of 4 μm to 16 μm, accounting for 89.5% of the total. Small starch granules smaller than 4 μm accounted for 2.3% of the total number, which was the smallest proportion. Large starch granules over 16 μm

accounted for 8.2% of the total number of granules, which were small in number but occupied most of the volume.

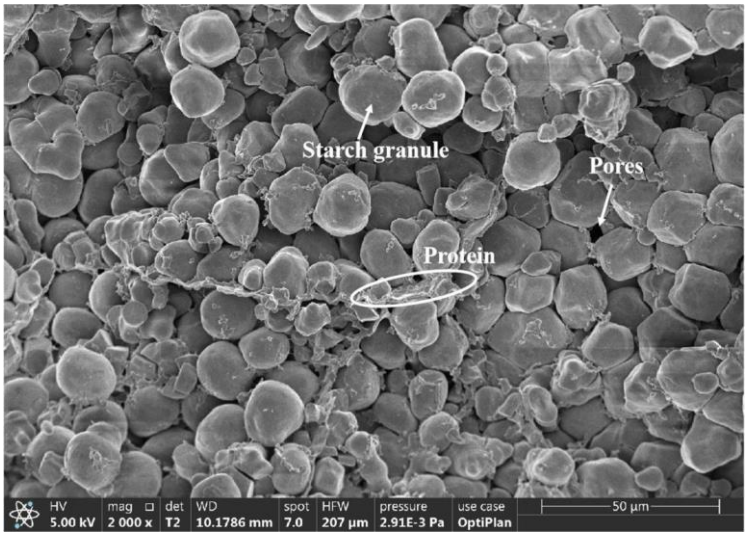

Figure 1. SEM images of powdered endosperm of corn kernels

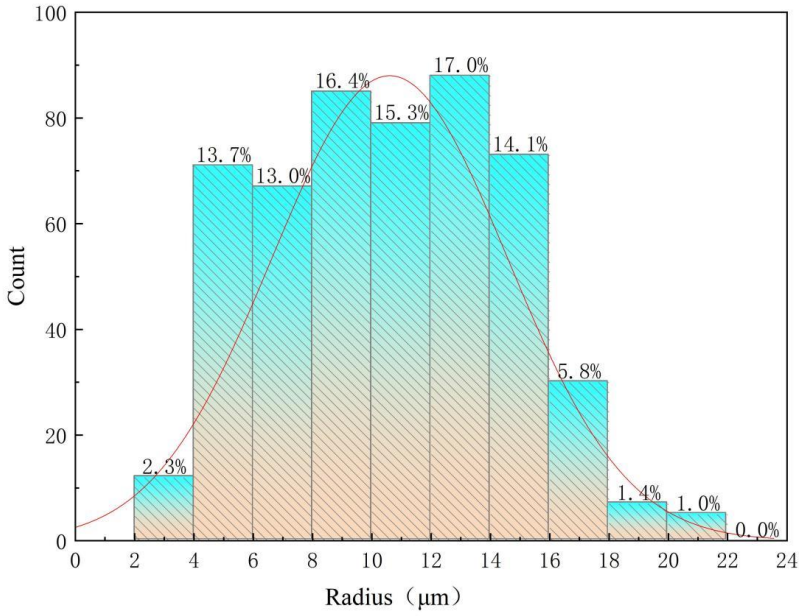

Figure 2. Particle size distribution of starch granules

III. Establishment of discrete element model of corn kernel powdery endosperm

In order to deeply investigate the causes of corn kernel crushing and the generation and expansion of cracks in the powdered endosperm portion of corn kernels at the microscopic scale, and taking into account the granular characteristics of the powdered endosperm of corn kernels at the microscopic scale, this section adopts PFC^{2D}, a discrete element software, which takes particles as the basic unit, to carry out modeling, and uses the microscopic parameters obtained from the SEM images as a reference to establish a discrete element model of the powdered endosperm portion of corn kernels at the microscopic scale, and after completing the establishment of the model, the model was loaded through the two-end loading plates to observe the generation and expansion of the microscopic cracks in the powdered endosperm portion of the corn kernels. The establishment of a discrete elemental model for the powdery endosperm fraction of corn kernels is divided into

two main steps: the selection of the contact model between starch granules, and the determination of the microsimulation parameters.

Principle of contact and choice of contact model

The powdery endosperm portion of the corn kernel is viewed on a microscopic scale, and the most basic unit constituting the endosperm is the starch granule. The starch granules are bonded together by proteins and other substances, but there are still pores between the starch granules, which have a certain effect on the mechanical properties between the starch granules. When force is applied to the powdery endosperm of corn kernels, the force on starch granules at the microscopic level is shown in Fig.3a, and there are two main ways of breaking the contact between starch granules as follows: tensile damage and shear damage for parallel bonded contacts.

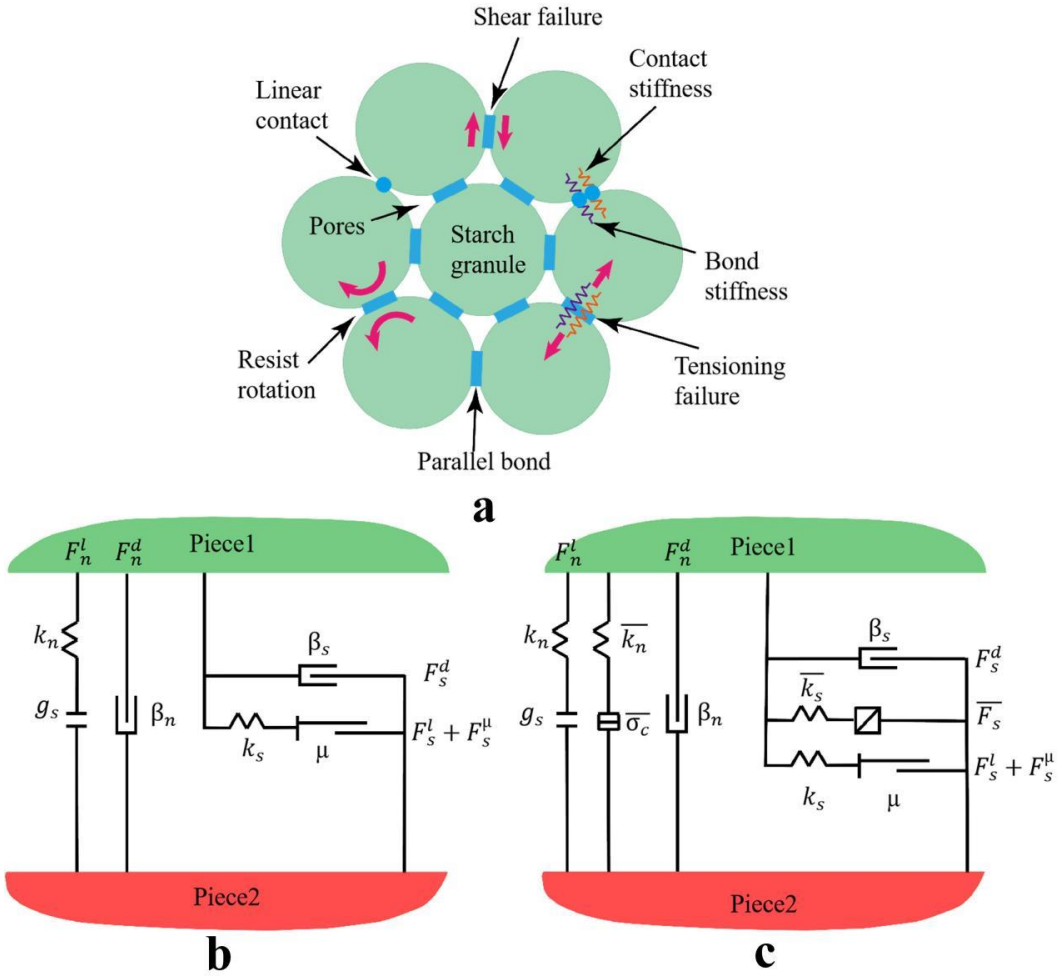

Figure .3 Starch intergranular contact principle diagram

If only the rigid contact between starch granules is considered, and the bonding effect of other substances such as proteins on starch granules is not taken into account, the contact mode between starch granules can be simply considered as a linear model, and the principle diagram of the linear contact model is shown in Fig.3b. k_n is the normal contact stiffness, k_s is the tangential contact stiffness, β_n and β_s represent the magnitude of the damping force in the normal and tangential directions, respectively, μ is the coefficient of friction in the shear direction, and g_s is the surface contact gap, and the linear model is activated when, and only when, the surface gap g_s is less than or equal to zero. The linear model contains a linear component and a damped component that act in parallel with each other, the two components act in the normal and tangential directions, respectively, the linear component provides linear elastic behavior but can only act under pressure and cannot withstand tension, while the damped component provides a viscous behavior, the model cannot resist relative rotation, so the contact moment Mc is zero in this model, and the mechanical behavior in the linear model can be described as follows:

$$F_c = F^l + F^d \quad (1)$$
$$M_c = 0 \quad (2)$$

Among them:

$$F^l = F_n^l + F_s^l \quad (3)$$
$$F^d = F_n^d + F_s^d \quad (4)$$
$$F_s^l = F_s^\mu = \mu F_n^l \quad (5)$$

F_c is the sum of contact force, the contact force is decomposed into linear force component F^l and damping force component F^d, M_c is the contact moment, F_n^l and F_s^l are the normal and tangential components of the linear force F^l, and F_n^d and F_s^d are the normal and tangential components of the damping force F^d, respectively.The value of F_s^l is equal to that of F_s^μ, the magnitude of F_s^μ is related to the friction coefficient μ and the normal force F_s^μ, and particle slip occurs when the force in the shear direction of the starch particle is greater than the maximum static friction. Obviously, it is not enough to consider only the linear interaction between the particles, because substances such as proteins have an obvious bonding effect on the starch particles, and to take this bonding behavior into account, it is necessary to add the bonding force between the proteins and other substances on the starch particles, and therefore to add a new force-parallel bonding force on the basis of the linear model, and the contact schematic diagram of the linear-parallel bonding contact model is shown in Fig.3b, and at this time, the mechanical behavior can be described as follows:

$$F_c = F^l + F^d + \bar{F} \quad (6)$$
$$\bar{M} = \bar{M}_t + \bar{M}_b \quad (7)$$
$$\bar{F} = \bar{F}_n + \bar{F}_s \quad (8)$$

$\bar{F}$ is the parallel bonding force, $\bar{F}$ can also be decomposed into normal parallel bonding force $\bar{F}_n$ and tangential parallel bonding force $\bar{F}_s$. In this model, the contact between starch granules is subjected to two kinds of forces, pressure and tension. When $\bar{F}_n$ is greater than 0, the contact between granules is subjected to pressure and vice versa to tension. $\bar{M}$ is the parallel bonding moment, which can be decomposed into torsional moment $\bar{M}_t$ and bending moment $\bar{M}_b$

Parallel bonding bond components and linear components act in parallel and establish elastic interactions between particles. Parallel bonding bond can be imagined as a set of elastic springs with constant normal and shear stiffness, uniformly distributed in the contact plane centered on the contact point of the two particles. The existence of the parallel bonding bond causes the starch granules to generate forces and moments at the contact, the magnitude of which is related to the maximum normal and shear stresses, and any of these maximum stresses exceeds the bond strength between the granules, and the parallel bonding bond breaks. After the parallel bonding bond breaks, the linear contact acts alone, at which time there is no moment acting between the particles, and it cannot resist relative rotation until the spacing g_s between the two particles is greater than zero, at which time the contact force disappears and the contact between the two particles disappears. As a result of these analyses, it can be concluded that the linear parallel bonded contact model best fits the actual mechanical properties of the powdered endosperm of corn kernels.

Determination of microscopic contact parameters and establishment of model

The establishment of the discrete element model of corn kernel powdery endosperm is mainly divided into five steps: particle generation, apply confining pressure, add cementation, unloading, and side loading plate removal. After the generation of the model, the upper and lower loading plates are loaded to observe the generation and propagation of mesoscopic cracks. Observing the powder endosperm starch particles through SEM images and modeling based on the actual size of corn starch particles, the particle size distribution of the modeling is shown in Table 1.

Table no 1 Particle gradation

Clusters	Particle size (μm)	Proportion(%)
1	2~4	2.3
2	4~8	26.7
3	8~12	31.7
4	12~16	31.1
5	16~18	5.8
6	18~22	2.4

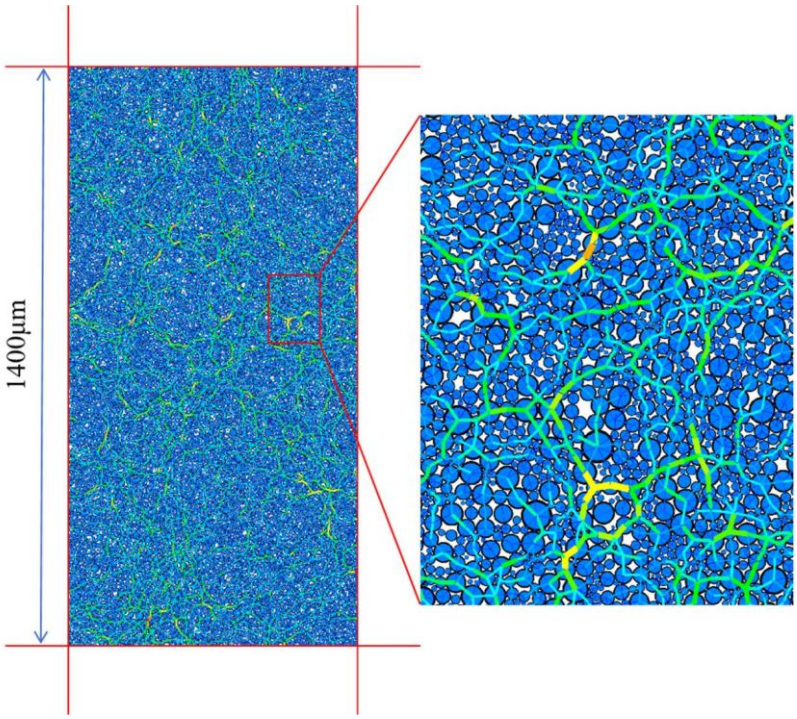

Figure .4 Discrete element model of floury endosperm

Taking the stress-strain curves obtained from the puncture experiments on the powdered endosperm portion of the corn kernel as a reference[11], the microscopic parameters in the model were calibrated after a series of trial-and-error methods, so that the loading simulation results of the established powdered endosperm discrete elemental model were more in line with the reality, and the microscopic parameters of the discrete elemental numerical model are shown in Table 2.

Table no 2 Model micro-parameters[17,18]

Parameter	Description	Value
$R_{max}/\mu m$	Maximum radius	2
$R_{min}/\mu m$	Minimum radius	22
$\rho/kg{\cdot}m^{-3}$	Density[endosperm part]	1300
emod	Effective modulus	1×10^7
kratio	Normal-to-shear stiffness ratio	1.5
pb-emod	Bond effective modulus	1×10^7
pb-kratio	Bond normal-to-shear stiffness ratio	1.5
fric	Friction coefficient	0.5
pb_coh/MPa	Cohesion [stress]	1×10^7
pb_ten/MPa	Tensile strength [stress]	3×10^7
porosity/%	Porosity	3

The height of the model boundary was set to be 1400 μm and the width to be 700 μm, the set parameters of the particle gradation were shown in Table 1, and the set parameters of the microscopic contact between the particles were shown in Table 2, and after the completion of the parameter setting, the discrete element simulation software generated a number of particles randomly and uniformly within the selected computational area. The model is created as shown in Fig.4, the number of particles generated by the model is 16370, the total number of contacts established between the particles is 27266, and the four red lines around the model are the four loading plates. The lines connecting the particles are force chains, and the thickness of the lines indicates the magnitude of the force.

After model generation the model needs to be pre-processed in four steps, apply confining pressure, add cementation, unloading, and side loading plate removal. The purpose of applying confining pressure is to bring the loose particles into close contact. The particles are generated randomly distributed in a set calculation area and are relatively loose, with no contact between the particles. The way to apply the confining pressure is to servo control the four loading plates, set the target stress of 10KPa for the four loading plates, each loading plate can independently detect the size of its own stress value, when the stress value is less than the target stress, the loading plate moves towards the internal direction of the model, squeezing the internal particles to increase the force between the particles, and when the stress value is greater than the target stress, the loading plate moves

outward until the size of the stresses on the four loading plates are in line with the target stresses. Although the particles are tightly stacked together after applying the confining pressure, the particles are not bonded to each other, but are simply in linear contact, at which time the particles are unable to resist rotational and tensile forces. It is necessary to add a parallel bonding bond between the particles, and this parallel bonding bond acts as an equivalent to the bonding of starch granules by substances such as proteins in the powdered endosperm of the corn kernel. After the contact relationship between the particles is established, the whole model can be unloaded slowly, and after the unloading is completed, the two sides of the loading plate are removed, at this time, the particles in the model will not disperse even without the action of the side loading plate force due to the bonding effect of the parallel bonding bonds, at this time, the establishment of the model is basically completed.

Model analysis

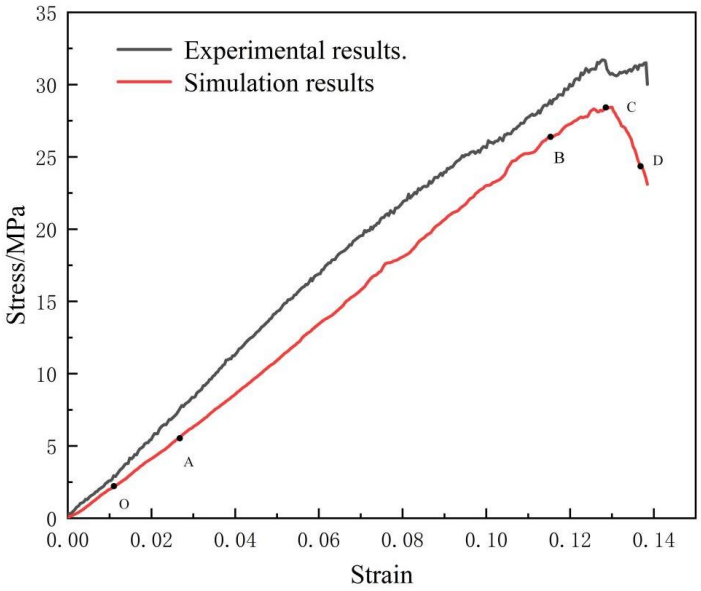

Figure .5 Stress-strain curve

The model was loaded in the displacement loading way, where the upper and lower loading plates loaded the model axially at a constant speed, and the loading was stopped when visible cracks appeared inside the model. When cracks appear inside and reach a certain number the stress magnitude on the upper and lower loading plates will show a rapid decrease, and the stress-strain curve during the loading process is shown in Fig.5. A comparison of the stress-strain curves of the powdered endosperm puncture experiment and the simulation results is given in Fig.5, and it can be seen that the stress-strain curves of the two are similar in shape, and the error is controlled within 10%, so the established model has some reference significance.

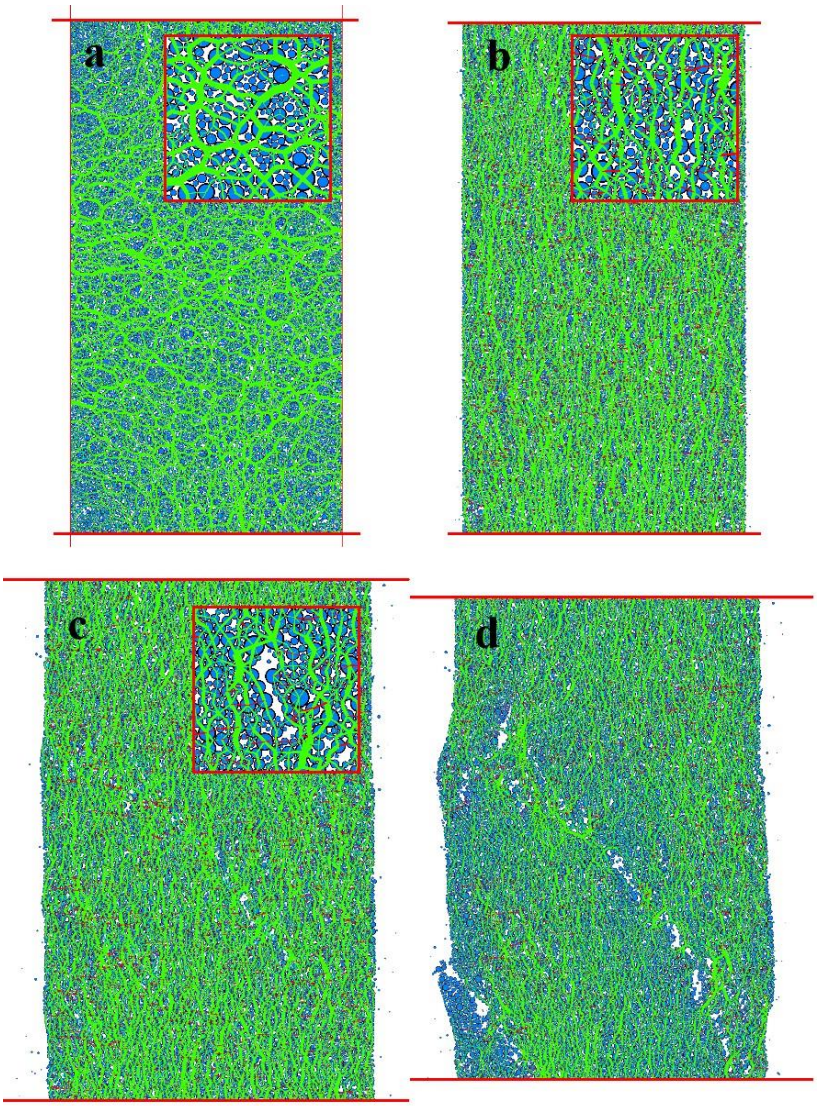

Figure .6 The process of model loading

The variation of the force chain during model loading is shown in Fig.6. The force between the particles is reflected by the force chains, the thickness of which reflects the magnitude of the force between the particles, where the force chains under pressure are green and those under tension are red. The whole loading process can be divided into four stages: initial, development, crack generation, and crack expansion, as shown in Fig.6, which correspond to the OA, AB, BC, and CD segments in the stress-strain curve of Fig.5, respectively.

The initial stage of loading is shown in Fig.6a, which corresponds to the OA segment in the stress-strain curve of Fig.5, when the stress on the loaded plate is small and the model strain is small. The number and thickness of the force chain in the model are distributed more uniformly, and the shape is similar to a fishing net, there is no obvious direction, at this time the force chain is mainly subject to pressure. As the loading plate continues to load the model, the model state goes from an initial stage to a developmental stage, as shown in Fig.6b, which corresponds to the AB segment in the stress-strain curve of Fig.5. At this time, the force chain appeared obvious directionality, the force chain direction for the loading plate loading principal stress direction, the shape is similar to the tree root-like, with the further increase of the force, the directionality of the force chain will be more obvious, at this time, the tensile force chain is gradually obvious. When reaching the BC section in Fig.5, the stress on the loading plate reaches a peak value of 28.5 MPa, corresponding to the crack generation stage in Fig.6c. At this stage the model has reached its load-bearing limit and the internal parallel bonding bonds begin to break down, starting to produce cracks of relatively small size and number. Continuing loading, the crack rapidly expands and becomes larger, as shown in Fig.6d, which is the crack expansion stage, corresponding to Fig.5CD segment. At this stage the force between the particles in the near vicinity of the crack exceeds the tolerance of the parallel bonding bonds, the parallel bonding bonds starts to break in large numbers and the crack expands rapidly to become larger and the stress on the loading plate decreases rapidly.

IV. Conclusion

(1) The microscopic morphology of the powdered endosperm portion of the corn kernel was obtained from SEM images, which provided parametric support for the establishment of a discrete Element Model of the powdered endosperm. The particle gradation in the model was determined from the actual particle sizes observed in the SEM images. By observing the bonding mode of starch particles in SEM images and analyzing the contact principle, the contact model-linear parallel bonding model was determined.

(2) A microscopic discrete element model of the powdery endosperm fraction of corn kernels was developed based on the discrete element software PFC^{2D}. There are four stages in the model loading process: initial, development, crack generation, and crack expansion. In the crack generation stage, the stress on the loaded plate reaches a peak value of 28.5 MPa, after which the loading continues and reaches the crack expansion stage, where the stress falls rapidly and cracks are produced in large quantities and expand rapidly

(3) The results of the simulations were validated by incorporating powdered endosperm puncture experiments. The stress-strain curves during model loading were similar to those obtained from the powdered endosperm puncture experiments, and the difference between the two peak stresses was within 10%, which verified the validity of the established discrete element model.

Funding: This research was funded by by the National Key Research and Development Program of China (2021YFD2000502), the Shandong Province Technology Innovation Capability Enhancement Project (2023TSGC0536), and the Key Research and Development Program of Rizhao (2023ZDYF010114).

References

[1]. Awika J M. Major Cereal Grains Production And Use Around The World[M]//Advances In Cereal Science: Implications To Food Processing And Health Promotion. American Chemical Society, 2011: 1-13.
[2]. Ranum P, Peña-Rosas J P, Garcia-Casal M N. Global Maize Production, Utilization, And Consumption[J]. Annals Of The New York Academy Of Sciences, 2014, 1312(1): 105-112.
[3]. Anderson T J, Lamsal B P. Zein Extraction From Corn, Corn Products, And Coproducts And Modifications For Various Applications: A Review[J]. Cereal Chemistry, 2011, 88(2): 159-173.
[4]. Xu W, Reddy N, Yang Y. Extraction, Characterization And Potential Applications Of Cellulose In Corn Kernels And Distillers' Dried Grains With Solubles (DDGS)[J]. Carbohydrate Polymers, 2009, 76(4): 521-527.
[5]. Ng H F, Wilcke W F, Morey R V, Et Al. Mechanical Damage And Corn Storability[J]. Transactions Of The ASAE, 1998, 41(4): 1095-1100.
[6]. Friday D, Tuite J, Stroshine R. Effect Of Hybrid And Physical Damage On Mold Development And Carbon Dioxide Production During Storage Of High-Moisture Shelled Corn[J]. Cereal Chemistry, 1989, 66(5): 422-426.
[7]. Teller R S, Schmidt R J, Whitlow L W, Et Al. Effect Of Physical Damage To Ears Of Corn Before Harvest And Treatment With Various Additives On The Concentration Of Mycotoxins, Silage Fermentation, And Aerobic Stability Of Corn Silage[J]. Journal Of Dairy Science, 2012, 95(3): 1428-1436.
[8]. Chulze S N. Strategies To Reduce Mycotoxin Levels In Maize During Storage: A Review[J]. Food Additives And Contaminants, 2010, 27(5): 651-657.
[9]. Chen Z, Wassgren C, Ambrose K. A Review Of Grain Kernel Damage: Mechanisms, Modeling, And Testing Procedures[J]. Transactions Of The ASABE, 2020, 63(2): 455-475.
[10]. Li X F, Jie X, Zhang Y L, Et Al. Detecting And Research On Characteristics And Mechanism Of Inner Mechanical Cracks Of Corn Seed Kernels[J]. Nongye Jixie Xuebao= Transactions Of The Chinese Society For Agricultural Machinery, 2010, 41(12): 143-147.
[11]. Wang B, Wang J. Mechanical Properties Of Maize Kernel Horny Endosperm, Floury Endosperm And Germ[J]. International Journal Of Food Properties, 2019, 22(1): 863-877.
[12]. Su Y, Cui T, Zhang D, Et Al. Damage Resistance And Compressive Properties Of Bulk Maize Kernels At Varying Pressing Factors: Experiments And Modeling[J]. Journal Of Food Process Engineering, 2019, 42(7): E13267.
[13]. Babić L J, Radojčin M, Pavkov I, Et Al. Physical Properties And Compression Loading Behaviour Of Corn Seed[J]. International Agrophysics, 2013, 27(2).
[14]. Chen Z, Wassgren C, Ambrose R P K. Measured Damage Resistance Of Corn And Wheat Kernels To Compression, Friction, And Repeated Impacts[J]. Powder Technology, 2021, 380: 638-648.
[15]. Singh S S, Finner M F, Rohatgi P K, Et Al. Structure And Mechanical Properties Of Corn Kernels: A Hybrid Composite Material[J]. Journal Of Materials Science, 1991, 26: 274-284.
[16]. Zhou W, Apkarian R, Wang Z L, Et Al. Fundamentals Of Scanning Electron Microscopy (SEM)[J]. Scanning Microscopy For Nanotechnology: Techniques And Applications, 2007: 1-40.
[17]. Meng F, Song J, Yue Z, Et Al. Failure Mechanisms And Damage Evolution Of Hard Rock Joints Under High Stress: Insights From PFC2D Modeling[J]. Engineering Analysis With Boundary Elements, 2022, 135: 394-411.
[18]. Ríos-Bayona F, Johansson F, Mas-Ivars D, Et Al. Using PFC2D To Simulate The Shear Behaviour Of Joints In Hard Crystalline Rock[J]. Bulletin Of Engineering Geology And The Environment, 2022, 81(9): 381.